C. elegans PAR-3 and PAR-6 are required for apicobasal asymmetries associated with cell adhesion and gastrulation

Jeremy Nance[1], Edwin M. Munro[2] and James R. Priess[1,*,†]

[1]Division of Basic Sciences, Fred Hutchinson Cancer Research Center, Seattle, WA 98109, USA
[2]Center for Cell Dynamics and Friday Harbor Labs, Friday Harbor, WA 98250, USA
*Howard Hughes Medical Institute, Seattle, WA 98109, USA
†Author for correspondence (e-mail: jpriess@fhcrc.org)

Accepted 23 July 2003

Development 130, 5339-5350
© 2003 The Company of Biologists Ltd
doi:10.1242/dev.00735

Summary

PAR proteins distribute asymmetrically across the anterior-posterior axis of the 1-cell-stage *C. elegans* embryo, and function to establish subsequent anterior-posterior asymmetries. By the end of the 4-cell stage, anteriorly localized PAR proteins, such as PAR-3 and PAR-6, redistribute to the outer, apical surfaces of cells, whereas posteriorly localized PAR proteins, such as PAR-1 and PAR-2, redistribute to the inner, basolateral surfaces. Because PAR proteins are provided maternally, distinguishing apicobasal from earlier anterior-posterior functions requires a method that selectively prevents PAR activity after the 1-cell stage. In the present study we generated hybrid PAR proteins that are targeted for degradation after the 1-cell stage. Embryos containing the hybrid PAR proteins had normal anterior-posterior polarity, but showed defects in apicobasal asymmetries associated with gastrulation. Ectopic separations appeared between lateral surfaces of cells that are normally tightly adherent, cells that ingress during gastrulation failed to accumulate nonmuscle myosin at their apical surfaces and ingression was slowed. Thus, PAR proteins function in both apicobasal and anterior-posterior asymmetry during the first few cell cycles of embryogenesis.

Movies available online

Key words: *C. elegans*, Apicobasal, PAR-3, PAR-6, NMY-2, Nonmuscle myosin, Gastrulation, Ingression, Cell adhesion

Introduction

Fertilization of the *C. elegans* egg initiates a cascade of events that defines the anterior-posterior axis of the embryo (reviewed by Pellettieri and Seydoux, 2002). Key components of this cascade are a group of proteins, collectively called PAR proteins, that associate asymmetrically with the cell cortex. PAR-3, PAR-6 and PKC-3 associate with the anterior cortex, whereas PAR-1 and PAR-2 associate with the posterior cortex (Boyd et al., 1996; Etemad-Moghadam et al., 1995; Guo and Kemphues, 1995; Hung and Kemphues, 1999; Tabuse et al., 1998). PAR functions are crucial for the subsequent anterior-posterior asymmetries of the early cells (reviewed by Kemphues and Strome, 1997). The anterior and posterior cells that arise from the first division of the egg differ in size, cleavage rate, spindle orientation, distribution of germline granules (P granules) and expression of several proteins, such as PIE-1, that are encoded by maternally provided mRNAs. *par* mutant embryos lack each of these asymmetries.

Although the PAR proteins have been studied primarily in newly fertilized, 1-cell embryos, they are expressed continuously during the early cell cycles and subsequently in epithelial cells during organogenesis. After the 1-cell stage, the anterior-posterior asymmetry of the PAR proteins is reiterated only in the lineage of cells that eventually produce the germline (germline precursors; see Fig. 1A). PAR-3, PAR-6 and PKC-3 associate with the anterior surface of each germline precursor prior to division, and PAR-1 and PAR-2 associate with the posterior surface (Boyd et al., 1996; Etemad-Moghadam et al., 1995; Guo and Kemphues, 1995; Hung and Kemphues, 1999; Tabuse et al., 1998). By contrast, the embryonic cells that produce only somatic cell types (somatic precursors) undergo a dramatic reorganization of PAR proteins (Boyd et al., 1996; Etemad-Moghadam et al., 1995; Guo and Kemphues, 1995; Hung and Kemphues, 1999; Nance and Priess, 2002; Tabuse et al., 1998). At the early 4-cell stage, the formerly anterior PAR proteins, PAR-3, PAR-6 and PKC-3, localize transiently to the entire cell cortex. By the late 4-cell stage, however, PAR-3, PAR-6 and PKC-3 redistribute to the contact-free, apical, surfaces of cells. The formerly posterior PAR proteins, PAR-1 and PAR-2, localize in a reciprocal manner to sites of cell contact, the basolateral surfaces. The PAR proteins gradually disappear from embryos after the 26-cell stage. PAR-3, PAR-6 and PKC-3 are expressed again at the ~400-cell stage in the epithelial cells of developing organs, where they are localized asymmetrically toward the apical surface (Leung et al., 1999; McMahon et al., 2001). The epithelial functions of the PAR proteins have not been studied in *C. elegans*. However, *Drosophila* homologs of PAR-3, PAR-6 and PKC-3 are expressed in epithelial cells where they appear to distinguish apical from nonapical membrane domains (reviewed by Knust and Bossinger, 2003). Mutations in the *Drosophila par* homologs result in gross defects in the polarity of epithelial cells and can cause epithelial cell sheets to become multilayered (Müller and Wieschaus, 1996; Petronczki and Knoblich, 2001; Wodarz et al., 2000).

What function might the PAR proteins perform in the interval between the 1-cell stage and organogenesis in *C. elegans* embryos? One possibility is that the anterior-posterior to apicobasal transition in PAR protein distribution has a role in gastrulation. During gastrulation, cells lack asymmetries typical of epithelial cells, such as localized adherens junctions and basement membranes, but have apicobasal asymmetries (Costa et al., 1998; Nance and Priess, 2002) (J.N., E.M.M. and J.R.P., unpublished). Gastrulation involves the movement, or ingression, of surface cells into the interior of the embryo (Nance and Priess, 2002; Sulston et al., 1983). Ingressing cells show a flattening and contraction of their apical surfaces and nonmuscle myosin becomes enriched at these surfaces (Lee and Goldstein, 2003; Nance and Priess, 2002). The ingressing cells move into a central cavity called the blastocoel. Blastocoel formation appears to involve specialization of the basal surfaces of cells, where PAR-2 and PAR-1 are located (Nance and Priess, 2002). By the end of the 4-cell stage small separations appear between cells along their innermost, basal surfaces; these separations increase in size over the next few cell cycles to form the blastocoel. Similar separations do not develop between the lateral surfaces of cells, which indicates that the lateral surfaces remain tightly adherent. Although the outer, apical surfaces of the early cells do not normally contact other cells, experiments on cultured embryos demonstrate that these surfaces also remain adhesive (Nance and Priess, 2002).

Previous studies have shown that the pattern of cell contacts in the early embryo determines the basal position of the blastocoel; 4-cell embryos that are combined head-to-head along their former apical surfaces generate an ectopic blastocoel between these surfaces (Nance and Priess, 2002). Interestingly, the PAR proteins have been shown to redistribute in these same experiments, with PAR-3 and PAR-6 moving to the new contact-free surfaces. Abnormal separations can develop between the lateral surfaces of cells in *par-3* and *par-6* mutants, but not *par-2* mutants, and cell ingressions are either absent or abnormal (Nance and Priess, 2002) (J.N., E.M.M. and J.R.P., unpublished). Thus, PAR-3 and PAR-6 might function in apicobasal asymmetry of early embryonic cells.

Determining whether PAR-3 and PAR-6 function in apicobasal asymmetry in the early embryo is complicated by their roles in anterior-posterior asymmetry at the 1-cell stage. For example, *par-3* mutant embryos have highly abnormal patterns of cell cleavage and altered cell fates that might disrupt apicobasal asymmetries indirectly (Kemphues et al., 1988). PAR-3 and PAR-6 are encoded by maternally supplied mRNAs (Kemphues et al., 1988; Watts et al., 1996), and the transition from anterior-posterior to apicobasal PAR asymmetry occurs without embryonic gene transcription (Nance and Priess, 2002). Thus, preventing PAR-3 and PAR-6 function after the 1-cell stage requires a method that selectively removes maternally supplied gene products.

In normal embryonic development, the maternal protein PIE-1 is distributed asymmetrically to the germline precursors, in part through the degradation of PIE-1 in somatic precursors (see Fig. 1A) (Mello et al., 1996; Reese et al., 2000). Analysis of PIE-1 has identified a peptide sequence, the ZF1 domain, which is necessary and sufficient for the degradation of PIE-1 in somatic precursors (Reese et al., 2000). Because the anterior-posterior asymmetry of the PAR proteins is established before the asymmetric degradation of PIE-1 (Tenenhaus et al., 1998), we reasoned that a PAR protein coupled to ZF1 might function in anterior-posterior asymmetry before being degraded. We show here that ZF1 coupled to PAR-3 and PAR-6 proteins rescue all the anterior-posterior defects associated with mutations in *par-3* and *par-6*, respectively. However, the coupled proteins disappear prior to gastrulation and the resulting embryos have defects in lateral adhesion and cell ingression. Thus, PAR-3 and PAR-6 have a role in apicobasal asymmetry in the early embryo that is independent of their earlier role in anterior-posterior asymmetry.

Materials and methods

Nematode strains and maintenance

Nematodes were cultured and manipulated genetically as described by Brenner (Brenner, 1974). The following mutant alleles and chromosomal rearrangements were utilized: chromosome I (LGI): *unc-101(m1)*, *par-6(zu222)* (Watts et al., 1996), *hIn*; LGIII: *lon-1(e185)*, *par-3(it71)* (Cheng et al., 1995), *unc-32(e189)*, *qC1*, *unc-119(ed3)*; LGIV: *spe-26(hc138*ts*)*, *him-8(e1489)*. Transgene insertions *zuIs20* (*par-3::zf1::gfp*), *zuIs52*, *zuIs54*, *zuIs57*, *zuIs58* (all *par-6::zf1::gfp*), *zuIs45* (*nmy-2::gfp*), *zuIs3* (*end-1::gfp*) and extrachromosomal array *zuEx69* (*par-6::gfp*) were created in this study and are described below. Additional references for mutations listed above can be found in (Hodgkin, 1997).

par-3(ZF1) strains were *lon-1 par-3; par-3::zf1::gfp(zuIs20); him-8. par-6(ZF1)* strains were *unc-101 par-6; par-6::zf1::gfp(zuIs54)*; other alleles of *par-6::zf1::gfp* were used where indicated. Because *par-3(ZF1)* and *par-6(ZF1)* strains were marked with *lon-1* and *unc-101* mutations, respectively, *lon-1* and *unc-101* worms were used as controls for these strains. The *him-8* mutation present in the *par-3(ZF1)* strain increases the frequency of males and does not alter early embryogenesis (Hodgkin et al., 1979) (J.N., E.M.M. and J.R.P., unpublished). A strain of genotype *unc-32 par-3; par-3::zf1::gfp(zuIs20)* was used to assess the viability of *par-3(ZF1)* embryos.

Plasmid construction

Standard techniques were used to manipulate and amplify DNA. Genomic sequences containing *par-3*, *par-6* and *nmy-2* were identified using the Wormbase web site (http://www.wormbase.org, release WS54, 2001). Cosmid DNA containing each gene was digested (*par-3*: F54E7, 16526 bp *Sal*I fragment; *par-6*: T26E3, 9080 bp *Xba*I-*Sma*I fragment; *nmy-2*: F20G4, 13965 bp *Xba*I fragment) and subcloned into the pBluescript KS+ vector (Stratagene). Subclones of each gene are predicted to include the entire coding region, 3′-untranslated region and 3-5 kb of sequence 5′ of the gene. A *Pst*I site was introduced either just before or in the stop codon of each gene by site-directed mutagenesis (Quickchange kit, Stratagene) or recombinant PCR. To construct *par-6::gfp* and *nmy-2::gfp*, the coding region of *gfp* was amplified by PCR from plasmid pPD95.75 (1995 Fire Lab vector kit, www.ciwemb.edu) and cloned into the introduced *Pst*I site. To construct *par-3::zf1::gfp* and *par-6::zf1::gfp*, sequences encoding the ZF1 domain (Reese et al., 2000) were first amplified by PCR from *pie-1* cDNA p661 (Mello et al., 1996) and introduced into the *Kpn*I site 5′ of *gfp* in plasmid pPD95.75; the resulting *zf1::gfp* coding region was amplified by PCR and cloned into the introduced *Pst*I site. Prior to transformation of each construct, the *unc-119*(+) coding region was inserted into the *Not*I site in the vector (Maduro and Pilgrim, 1995).

To construct *end-1::gfp*, the *end-1* promoter (2126 bp 5′ to 75 bp 3′ of the *end-1* start codon) was amplified by PCR and fused 5′ of *gfp* coding sequences in plasmid pPD95.75 (Cassata et al., 1998).

Worm transformations

Strains expressing *par-3::zf1::gfp, par-6::gfp, par-6::zf1::gfp* and *nmy-2::gfp* were obtained by microparticle bombardment of *unc-119* worms with plasmids described above (Praitis et al., 2001). A strain expressing the *end-1::gfp* reporter was obtained by injecting *spe-26* worms with *end-1::gfp* and a *spe-26*(+) cotransformation marker; the resulting *end-1::gfp* extrachromosomal array was integrated by γ-irradiation (Mello and Fire, 1995).

Antibodies and immunostaining

Anti-PAR-3 monoclonal antibody P4A1 was produced in collaboration with Ken Kemphues. Purified recombinant PAR-3 (Etemad-Moghadam et al., 1995) was injected into mice at the FHCRC Hybridoma Production Facility as described (Wayner and Carter, 1987). Hybridoma supernatants were assayed by immunostaining early embryos fixed in bulk with paraformaldehyde and methanol (Costa et al., 1997). Antibody P4A1 stained early embryos in the same pattern as previously described PAR-3 polyclonal sera (Etemad-Moghadam et al., 1995) and did not stain either *par-3(it71)* or *par-3(RNAi)* early embryos (data not shown).

For most immunostaining experiments, embryos were fixed on slides using the freeze-crack methanol procedure and incubated with primary antibodies and fluorochrome-conjugated secondary antibodies (Leung et al., 1999); embryos were fixed for PIE-1 immunostaining as described (Mello et al., 1996). The following primary antibodies/antisera and dilutions were used: chicken anti-GFP, 1:200 (Chemicon); mouse anti-HMP-1, 1:10 (Costa et al., 1998); rabbit anti-HMR-1, 1:10 (Costa et al., 1998); rabbit anti-LAD-1, 1:300 (Chen et al., 2001); rabbit anti-PAR-1, 1:30 (Guo and Kemphues, 1995); rabbit anti-PAR-2, 1:3 (Boyd et al., 1996); mouse anti-PAR-3, 1:20 (this study); rabbit anti-PAR-6, 1:20 (Hung and Kemphues, 1999); mouse anti-PIE-1, 1:10 (Mello et al., 1996); rat anti-PKC-3, 1:10 (Tabuse et al., 1998); rabbit anti-PGL-1, 1:1000 (Kawasaki et al., 1998). Images of immunostained embryos were captured on a Deltavision microscope (Applied Precision) and deconvolved. Where not indicated, immunostaining observations were based on the analysis of >15 embryos at the appropriate stage.

Chimeric embryos

Embryos were combined, cultured and immunostained for PAR-3 as described (Nance and Priess, 2002). Wild-type and *par-3* mutant embryos were combined at the 2-cell stage such that the anterior cell of the wild-type embryo contacted a *par-3* mutant cell. Chimeric embryos were cultured for 2-3 division cycles before fixation. Wild-type cells were recognized by their distinctive pattern of cell division and the presence of cortical PAR-3.

Electron microscopy

lon-1 par-3; par-3::zf1::gfp; him-8 and control *lon-1* embryos were fixed and processed for electron microscopy as described (Priess and Hirsh, 1986). For each genotype, sections of 40-50 fixed embryos at the 12-15 cell stage were analyzed.

Imaging and analysis of live embryos

Embryos were mounted and imaged for 3D-timelapse microscopy as described (Nance and Priess, 2002). Fluorescence images of embryos expressing GFP were acquired on a Leica TCS scanning confocal microscope.

Reported cell division times are in minutes from the beginning of the 2-cell stage. Times were normalized to those reported by Sulston et al. (Sulston et al., 1983). Initiation of ingression of mesodermal cells was scored when these cells first began to sink below the surface of the embryo.

nmy-1 RNA-mediated interference

Double-stranded RNA (dsRNA) corresponding to bases 5425-5889 of the *nmy-1* cDNA was synthesized as described (Nance and Priess, 2002). Young adult hermaphrodites were injected with *nmy-1* dsRNA (3.5 μg μl^{-1}) and 24 hours later eggs at the 1-4 cell stage were collected, mounted and video-recorded for 150 minutes as described above. Ingression of endodermal cells was analyzed as described in the legend to Table 1. Endodermal cells failed to ingress within the recording period in 1 out of 12 *nmy-1(RNAi)* embryos; reported ingression times are for the remaining 11 embryos. Although it was not possible to monitor NMY-1 protein levels to quantitatively determine the efficacy of RNAi, all injected control

Table 1. Phentoypes of control and *par(ZF1)* embryos

Embryo genotype*	GFP levels†	Equal division	Cell cycle length (minutes)‡		Lateral spaces§		Endoderm internal (minutes)¶
			MS(2) to MS(4)	E(2) to E(4)	Surface	Interior	
Wild type (WT)	NA	0/13	24.2±0.7 (3)	44.3±3.0 (3)	0/8	0/8	113±6.2 (8)
par-3(ZF1)	++	0/98	24.7±0.8 (8)	45.5±1.7 (8)	7/10	7/10	141±6.0 (8)
WT+*par-3::zf1::gfp*	++	ND	ND	ND	0/3	1/3	110±6.9 (3)
par-3(–)	NA	15/15	NA	NA	ND	ND	NA
WT	NA	0/17	24.8±0.6 (6)	46.2±1.3 (6)	0/6	1/6	112±6.7 (6)
par-6(ZF1) (total)	NA	0/129	24.5±0.4 (14)	46.7±0.2 (14)	7/14	8/14	133±7.5 (14)
par-6(ZF1) (zuIs57)	++++	0/34	24.1±0.9 (3)	46.3±1.1 (3)	1/3	2/3	132±12 (3)
par-6(ZF1) (zuIs58)	++++	0/34	24.4±1.0 (4)	47.0±1.6 (4)	3/4	4/4	131±6.4 (4)
par-6(ZF1) (zuIs54)	+++	0/31	24.5±0.6 (3)	46.8±1.9 (3)	0/3	2/3	135±5.1 (3)
par-6(ZF1) (zuIs52)	+	0/30	25.0±0.3 (4)	46.6±1.5 (4)	3/4	2/4	136±4.5 (4)
WT+*par-6::zf1::gfp*	++++	ND	ND	ND	0/4	1/4	113±8.9 (4)
par-6(–)	NA	13/13	NA	NA	ND	ND	NA

NA, not applicable; ND, not determined.

**lon-1* worms were used as wild-type controls for *par-3(ZF1)* strains, and *unc-101* worms were used as wild-type controls for *par-6(ZF1)* strains. Alleles of *par-6::zf1::gfp* in *par-6(ZF1)* strains are indicated in parentheses; the sum or average of all *par-6(ZF1)* alleles is indicated by '(total)'. See Materials and methods for additional notes on genotype.

†GFP expression levels were examined in live embryos. ++++ embryos, GFP visible beyond the four-cell stage; +++ embryos, GFP visible up to the four-cell stage; ++ embryos, GFP visible up to the two-cell stage; + embryos, GFP detected by camera but not eye at the two-cell stage.

‡The MS(2) to MS(4), and E(2) to E(4) cell cycle lengths refer to the interval between the first and second divisions of the MS and E cells, respectively. Values are averages±s.d. (sample size).

§Lateral spaces were scored either from focal planes at the interior of embryos at the 15-cell stage, or from the surface of embryos between the six- and 24-cell stages. Only perduring separations >1 μm present between interphase cells were scored as lateral spaces.

¶Values are averages±s.d. (sample size) in minutes after the two-cell stage and indicate when the endodermal cells were internal (completely covered by surface cells).

(*lon-1*) embryos displayed defects in the elongation stage of embryogenesis (*n*=20).

Results

PAR-3$^{ZF1\text{-}GFP}$ and PAR-6$^{ZF1\text{-}GFP}$ are degraded in somatic cells

To examine the role of *par-3* and *par-6* in the apicobasal polarity of early embryonic cells, we first constructed *par-6::zf1::gfp* and *par-3::zf1::gfp* transgenes, and a control *par-6::gfp* transgene. These transgenes were integrated into chromosomes using techniques that allow stable expression in the germ line (see Materials and methods). The PAR-3$^{ZF1\text{-}GFP}$ and PAR-6$^{ZF1\text{-}GFP}$ proteins encoded by the transgenes were localized to the anterior cortex of 1-cell embryos in a pattern indistinguishable from that of the normal PAR-3 and PAR-6 proteins, and control PAR-6^{GFP} protein (Fig. 1Ba,b). At each cell cycle after the 1-cell stage, the embryo consists of one or more somatic precursor cells (Fig. 1A, cells outlined in bold) and one germline precursor (Fig. 1A, dark red cells). At each stage, the PAR-6$^{ZF1\text{-}GFP}$ and PAR-3$^{ZF1\text{-}GFP}$ proteins showed an anterior-posterior asymmetry in the germline precursor that was indistinguishable from normal PAR-3 and PAR-6 proteins (Fig. 1Bc,d, small arrows). Therefore, PAR proteins that are linked to the ZF1 domain reproduce the normal anterior-posterior asymmetries of the PAR-3 and PAR-6 proteins in the 1-cell embryo and in germline precursors at subsequent stages.

In contrast to the germline precursors, the levels of PAR-3$^{ZF1\text{-}GFP}$ and PAR-6$^{ZF1\text{-}GFP}$ in somatic precursors diminished to undetectable levels. During the 4-cell stage, when PAR-3, PAR-6 and PAR-6^{GFP} redistributed to the apical cortices of all three somatic precursors (Fig. 1Bc, large arrow, and data not shown), PAR-3$^{ZF1\text{-}GFP}$ was absent in the two oldest somatic precursors (the ABa and ABp cells; Fig. 1Bd, large arrow). In EMS, the youngest somatic precursor, PAR-3$^{ZF1\text{-}GFP}$ began to redistribute from the cell periphery to the apical cortex (Fig. 1Bd, arrowhead), but disappeared during the following cell cycle. PAR-6$^{ZF1\text{-}GFP}$ disappeared similarly in the somatic precursors, but usually required an additional cell cycle to do so (Fig. 1Bf). After the 4-cell or 8-cell stages, PAR-3$^{ZF1\text{-}GFP}$ and PAR-6$^{ZF1\text{-}GFP}$ could not be detected in the older somatic precursors by either GFP fluorescence or immunostaining for GFP. For example, at the 26-cell stage, when the endodermal precursors normally begin the first cell ingressions, PAR-3$^{ZF1\text{-}GFP}$ and PAR-6$^{ZF1\text{-}GFP}$ were not detected in the endodermal precursors or the neighboring cells that flank the anterior and lateral sides of the endodermal precursors (Fig. 1Bh and data not shown).

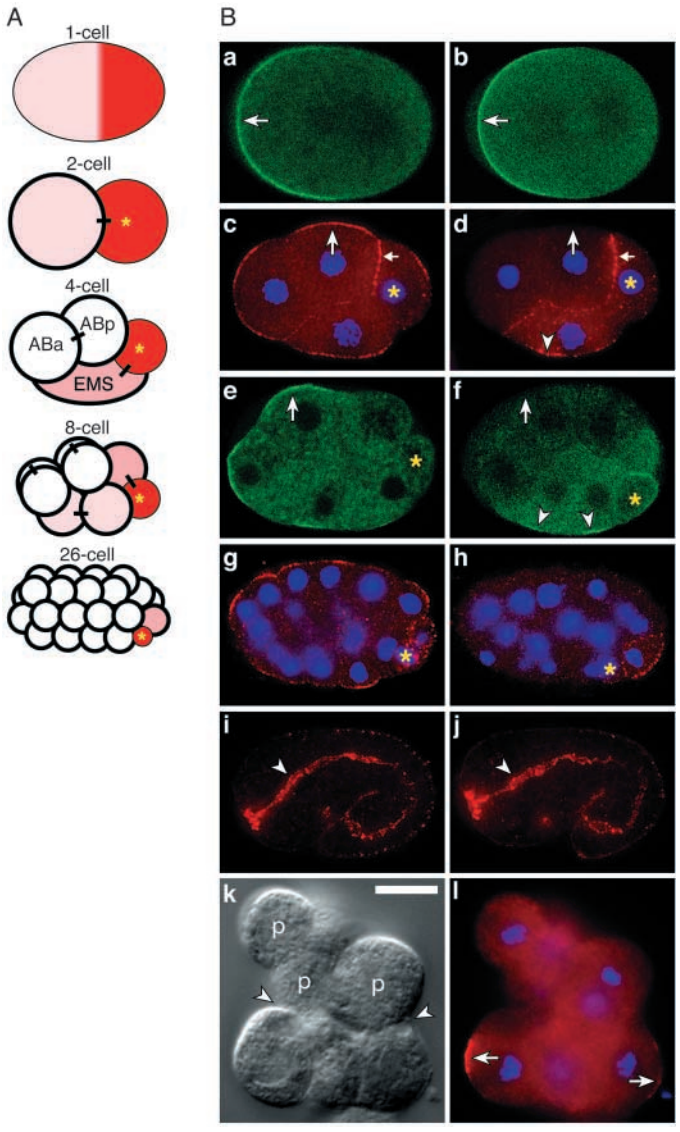

Fig. 1. Localization and degradation of PAR proteins. (A) Schematic diagram of early stages of embryogenesis; sister cells are linked by short bars. Somatic precursors are indicated by bold outlines, germline precursors are indicated by a yellow asterisk. Germline precursors divide asymmetrically into a somatic precursor and a new germline precursor; the germline daughter has a high level of germline proteins, such as PIE-1, (dark red cells) and the somatic daughter contains a low level of PIE-1 (pink cells) that is degraded within one or two additional cell cycles (white cells). (B) PAR expression in early embryos. Embryos are oriented as in panel A; yellow asterisks mark germline precursors. (a,b) 1-cell embryos expressing either PAR-6^{GFP} (a) or PAR-6$^{ZF1\text{-}GFP}$ (b); arrows point to the anterior cortex. (c,d) 4-cell embryos stained for endogenous PAR-3 (c) or PAR-3$^{ZF1\text{-}GFP}$ (d); large arrow in c points to the apical cortex of ABp. (d) Large arrow in d indicates the apical cortex of ABp, arrowhead indicates the apical cortex of EMS, and small arrow points to the cortex of the germline precursor. (e,f) 8-cell embryos expressing either PAR-6^{GFP} (e) or PAR-6$^{ZF1\text{-}GFP}$ (f); note that PAR-6$^{ZF1\text{-}GFP}$ has disappeared from the oldest somatic cells (arrow) but is still detectable in the younger somatic cells (arrowheads). (g,h) 24-cell embryos showing PAR-3 (g) and PAR-3$^{ZF1\text{-}GFP}$ (h). (i,j) PAR-3 expression in epithelia of an organogenesis-stage wild-type embryo (i) and a *par-3(ZF1)* embryo (j); arrowheads point to the apical surfaces of cells forming the digestive tract. (k) Chimeric embryo formed by combining a wild-type embryo with a *par-3* mutant embryo; arrowheads indicate former apical surfaces of the wild-type cells that now contact the *par-3* mutant cells (*p*). (l) PAR-3 expression in the chimeric embryo in k; note localization of PAR-3 to the contact-free surface of the wild-type cell (arrows). In all panels, exposures were adjusted to visualize the background fluorescence of cells; the level of fluorescence in the ABa and ABp cells in d was similar to that in *par-3* mutant embryos lacking the transgene. Transgene expression was identical in wild-type and *par-3* mutant backgrounds; embryos shown are wild-type in a-c,e-g,i and *par-3* in d,h,j. Embryos in this and subsequent figures are ~50 μm in length. Scale bar: 10 μm.

Although normal embryos express PAR-3 and PAR-6 until the 26-cell stage (Fig. 1Bg and data not shown), the levels of these proteins gradually decline during subsequent cell cycles. A second phase of expression coincides with the beginning of organogenesis (~400-cell stage), when PAR-3 and PAR-6 appear in nascent epithelial cells (Fig. 1Bi and data not shown). We found that PAR-3$^{ZF1\text{-}GFP}$ and PAR-6$^{ZF1\text{-}GFP}$ were expressed in nascent epithelia in a pattern similar to that of endogenous PAR-3 and PAR-6 (Fig. 1Bj and data not shown). This result indicates that the machinery that degrades proteins with the ZF1 domain does not operate at the 400-cell and later stages. In summary, we conclude that the ZF1 domain effectively removes the PAR-3$^{ZF1\text{-}GFP}$ and PAR-6$^{ZF1\text{-}GFP}$ proteins from somatic precursors between the 4- and 8-cell stages until the beginning of organogenesis.

par::zf1::gfp transgenes restore anterior-posterior asymmetry to *par* mutant embryos

To test whether the PAR-3$^{ZF1\text{-}GFP}$ and PAR-6$^{ZF1\text{-}GFP}$ proteins could provide PAR functions essential for anterior-posterior asymmetry, we crossed the corresponding transgenes into *par-3* or *par-6* mutant strains, which lack detectable maternal PAR-3 or PAR-6, respectively (Etemad-Moghadam et al., 1995; Hung and Kemphues, 1999). For simplicity, we refer to a *par-3* mutant with an integrated *par-3::zf1::gfp* transgene as *par-3(ZF1)*, and to *par-3(ZF1)* and *par-6(ZF1)* embryos collectively as *par(ZF1)* embryos. Although the *par-3(ZF1)* and *par-6(ZF1)* embryos had abnormalities in the appearance of early embryonic cells and in cell movements during gastrulation (see below), most of the embryos developed to hatching and grew to fertile adults [eggs hatched in wild type, 1271/1281 (99%); *par-3(ZF1)*, 1061/1085 (98%); *par-6(ZF1)*, 2443/2548 (96%)]. The *par-6(ZF1)* strain with the lowest level of PAR-6$^{ZF1\text{-}GFP}$ expression (*zuIs52*, see Table 1) produced some embryos that grew to agametic adults (30/396). This phenotype has been described in strains with hypomorphic alleles of *par-3* and *par-6*, and is likely to reflect suboptimal levels of PAR-6$^{ZF1\text{-}GFP}$ in germline cells (Kemphues et al., 1988; Watts et al., 1996).

PAR-6$^{ZF1\text{-}GFP}$ was expressed asymmetrically at the 1-cell stage and in the germline precursors in *par-6(ZF1)* embryos and wild-type embryos, and similar results were observed for PAR-3$^{ZF1\text{-}GFP}$ in *par-3(ZF1)* embryos (Fig. 1Ba,b and data not shown). Thus, the ZF1-tagged proteins provide sufficient *par-6(+)* or *par-3(+)* function to promote their own asymmetric localization. We asked whether the anterior-posterior asymmetries that characterize the first division of a wild-type embryo occurred in the *par(ZF1)* embryos. The first division is unequal in wild-type embryos (Fig. 2A), resulting in a small posterior daughter (the germline precursor), but in *par-3* and *par-6* mutant embryos the first division is equal (Fig. 2E, Table 1). In all *par(ZF1)* embryos examined the first cell division was unequal, as in wild-type embryos (Fig. 2I, Table 1). Similarly, the subsequent three divisions of the germline precursors were unequal in the *par(ZF1)* embryos, as in wild-type embryos (wild type, *n*=14; *par-3(ZF1)*, *n*=15; *par-6(ZF1)*, *n*=14). In wild-type embryos, the first division results in the asymmetric localization of PIE-1 and cytoplasmic granules, called P granules, to the posterior daughter (Fig. 2B,C). These asymmetries are absent in *par-3* and *par-6* mutant embryos (Fig. 2F,G), but were present in all *par-3(ZF1)* and *par-6(ZF1)* embryos (Fig. 2J,K) (P granules: wild type, *n*=54; *par-3(ZF1)*, *n*=26; *par-6(ZF1)*, *n*=62. PIE-1: wild type, *n*=58; *par-3(ZF1)*, *n*=35; *par-6(ZF1)*, *n*=44).

Each of the early cells has a distinctive cell-cycle period in wild-type embryos, whereas all the early divisions are approximately synchronous in *par* mutant embryos. We determined the cell-cycle periods for each cell through the 50-cell stage in *par-3(ZF1)* and *par-6(ZF1)* embryos and found these to be indistinguishable from wild type (Table 1 and data not shown). In normal embryogenesis, the descendants of the E cell, and no other cells, express an endoderm-determining

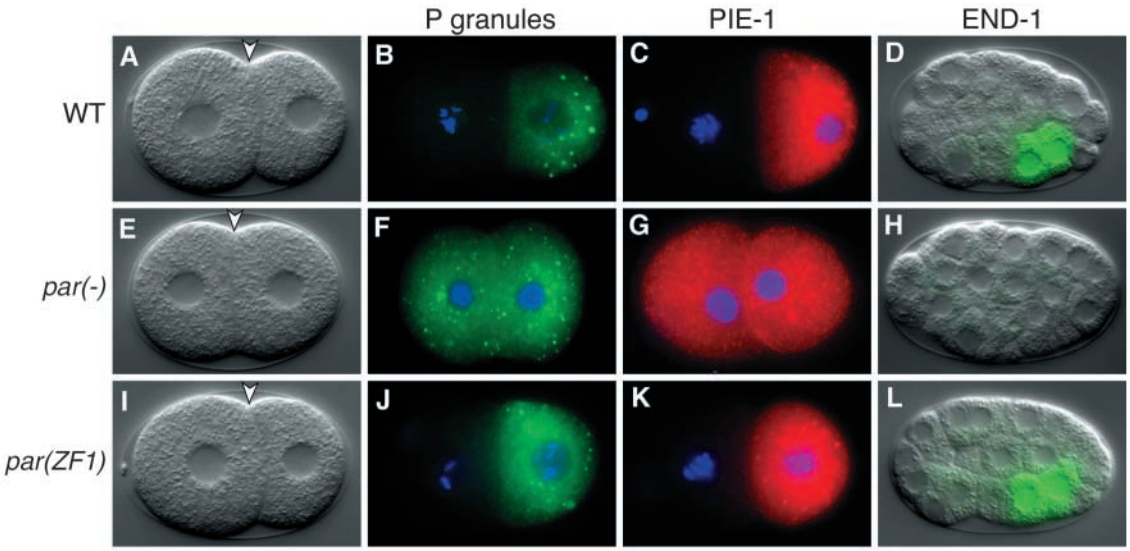

Fig. 2. Anterior-posterior asymmetry. (A-D) Wild-type, 2-cell embryo in the light microscope (A) after staining for P granules (B, green), and PIE-1 (C, red). DNA is shown in blue. (D) A 24-cell, wild-type embryo with an *end-1::gfp* transgene; the GFP fluorescence image (green) was superimposed on the light microscope image. The middle and bottom rows show *par*-mutant embryos (middle) and *par(ZF1)* embryos (bottom) prepared as above. Embryo genotypes are as follows: *par-3(it71)* (E,F,H); *par-6(zu222)* (G); *par-3(ZF1)* (I,J,L); *par-6(ZF1)* (K).

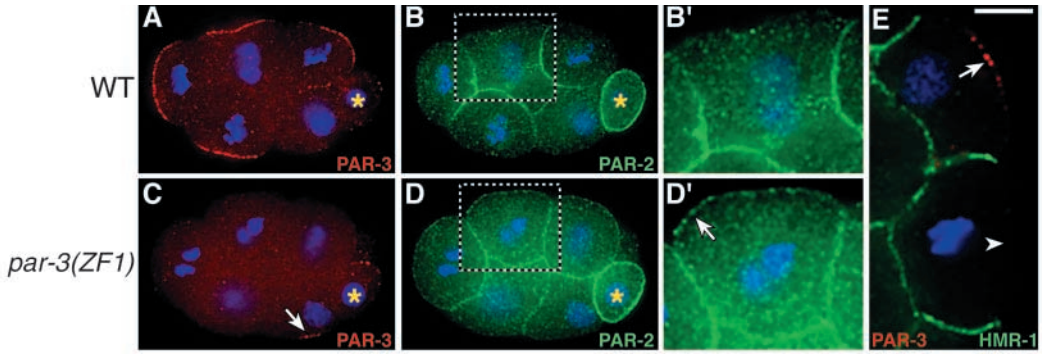

Fig. 3. Localization of PAR-2 and HMR-1/E-cadherin. (A-D) Each row shows a single 8-cell embryo, either wild-type or *par-3(ZF1)*, immunostained for both PAR-3 (A,C) and PAR-2 (B,D). (B′,D′) higher magnifications of the boxed regions in B,D, respectively. The arrow in C points to PAR-3 that remains in a young somatic cell. Note presence of apical PAR-2 in the *par-3(ZF1)* embryo (arrow in D′). (E) Two cells in an 8-cell *par-3(ZF1)* embryo immunostained for PAR-3 (red) and HMR-1 (green). PAR-3 is present at the apical cortex (arrow) of one cell only. Note that HMR-1 is present at basolateral surfaces but is not detected at apical surfaces (arrowhead). DNA is stained blue in all panels. Yellow asterisks mark germline precursors. Scale bar: 5 μm.

factor called END-1; this asymmetry results from the combination of asymmetrically localized transcriptional regulators and asymmetric cell-cell interactions (reviewed by Maduro and Rothman, 2002). Wild-type and *par-3(ZF1)* embryos both showed correct expression of an *end-1::gfp* transgene only in the E daughters (Fig. 2D,L), whereas *par-3* embryos either lacked *end-1::gfp* expression or had faint expression in multiple cells (n=30) (Fig. 2H). Taken together, these observations indicate that the expression of a *par::zf1::gfp* transgene in a *par* mutant embryo fully rescues defects in anterior-posterior asymmetry.

PAR localization in *par(ZF1)* embryos

PAR$^{ZF1\text{-}GFP}$ proteins were degraded rapidly in the somatic precursor cells of the *par(ZF1)* strains in a pattern similar to the degradation of PAR$^{ZF1\text{-}GFP}$ proteins in otherwise wild-type strains (Fig. 1Bc-h, Fig. 3C). Because degradation of the PAR$^{ZF1\text{-}GFP}$ proteins occurred progressively with the age of the somatic precursor, we observed several examples where a cell with apical PAR$^{ZF1\text{-}GFP}$ was adjacent to a cell that lacked PAR$^{ZF1\text{-}GFP}$. This pattern indicates that apical restriction of PAR-3 does not require PAR-3-mediated interactions with neighboring cells. To test this hypothesis further, we combined wild-type embryos with *par-3* mutant embryos at the 2-cell stage and allowed the chimeric embryos to divide in culture. In each of seven chimeric wild-type/*par-3* mutant embryos, PAR-3 was excluded from all surfaces where a wild-type cell contacted a *par-3* mutant cell. Instead, PAR-3 was concentrated on the contact-free surfaces of the wild-type cells (Fig. 1Bk,l and Discussion). These results are similar to those of a previous study where wild-type embryos were combined with wild-type embryos (Nance and Priess, 2002) (data not shown).

Genetic studies have shown that the localization of PAR proteins in the 1-cell embryo is interdependent; removal of any one protein can alter the pattern of, or prevent, the cortical localization of the other PAR proteins (Boyd et al., 1996; Etemad-Moghadam et al., 1995; Hung and Kemphues, 1999; Tabuse et al., 1998; Watts et al., 1996). We therefore asked whether the apicobasal localization of the PAR proteins after the 1-cell stage involved a similar interdependence. PAR-1 and PAR-2 are normally associated with the basolateral surfaces of somatic precursors (Fig. 3B,B′ and data not shown). After the degradation of either PAR-3$^{ZF1\text{-}GFP}$ or PAR-6$^{ZF1\text{-}GFP}$ in the somatic precursors of *par(ZF1)* embryos, PAR-1 and PAR-2 localized to both the apical and basolateral surfaces (Fig. 3D,D′ and data not shown). Thus PAR-3 and PAR-6 functions appear to be required to restrict PAR-1 and PAR-2 to the basolateral surfaces.

We next asked if the apical localizations of PAR-3, PAR-6 and PKC-3 were interdependent. The youngest somatic cells of *par-3(ZF1)* embryos contained apical PAR-3$^{ZF1\text{-}GFP}$ (Fig. 4C, arrow) and PKC-3 colocalized with PAR-3$^{ZF1\text{-}GFP}$ (Fig. 4D, arrow). The older somatic cells lacked PAR-3$^{ZF1\text{-}GFP}$ and contained cytoplasmic rather than apical PKC-3 (Fig. 4D). Similarly, PKC-3 also failed to localize to the apical cortex in the somatic cells lacking PAR-6$^{ZF1\text{-}GFP}$ in *par-6(ZF1)* embryos (Fig. 4E,F). By contrast, endogenous PAR-3 showed a robust association with the apical cortex of cells lacking PAR-6$^{ZF1\text{-}GFP}$ in *par-6(ZF1)* embryos (Fig. 4G,H). The apical localization of PAR-3 in the *par-6(ZF1)* strain does not result simply from the perdurance of cortical PAR-3 after the degradation of PAR-6$^{ZF1\text{-}GFP}$: in both wild-type embryos and in *par-6(ZF1)* embryos, PAR-3 disappeared transiently from the cortex during cell division and reappeared during the next cell cycle. In summary, PAR-3, but not PKC-3, associates specifically with the apical cortex in cells that lack PAR-6. However, neither PAR-6 nor PKC-3 can associate with the apical cortex of cells that lack PAR-3.

Cell-cell adhesion and ingression are defective in *par(ZF1)* embryos

In early wild-type embryos the lateral, but not basal, surfaces of interphase cells are tightly adherent. We reported previously that *par-3* mutant embryos have abnormally large spaces between the lateral surfaces of cells (Nance and Priess, 2002). We therefore examined cell-cell contacts in video recordings of *par-3(ZF1)* and *par-6(ZF1)* embryos. Embryos from both strains developed separations between the basal surfaces of cells to form a central blastocoel. However, additional, large separations were present between the lateral surfaces of cells in the *par(ZF1)* embryos (Fig. 5C, Table 1) but not wild-type embryos (Fig. 5A, Table 1). Focal planes through the *par(ZF1)* embryos often showed abnormal spaces 1-2 μm wide between the otherwise contiguous lateral surfaces of cells (Fig. 5D, Table 1). Electron microscopy confirmed that the images visible in the light microscope were intercellular spaces rather than intracellular structures (Fig. 5E). We consider it

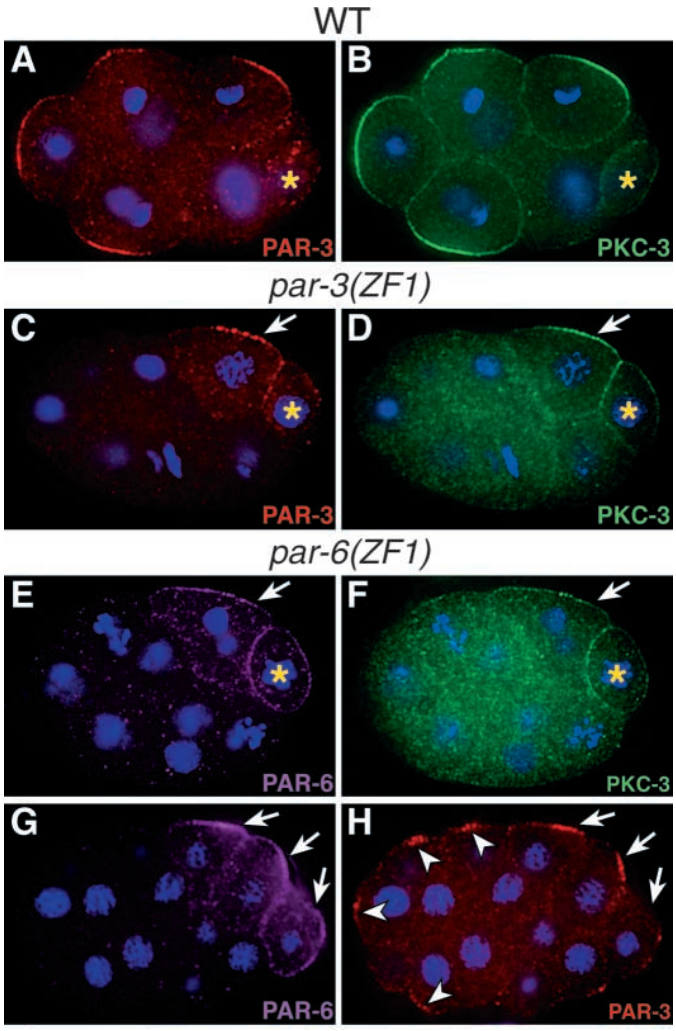

Fig. 4. Localization of apical PAR proteins. Each row depicts a single embryo immunostained for the protein at the bottom right of each panel. Embryo genotypes are shown above each row. Where visible, the germline precursor is indicated with a yellow asterisk and the youngest somatic precursors are indicated by arrows. Embryos are shown at representative stages; similar results were obtained for other stages. (A-B) An 8-cell embryo. (C-D) A 12-cell embryo. (E-F) A 14-cell embryo. (G-H) A 26-cell embryo. At this stage, PAR-3$^{ZF1\text{-}GFP}$ is present only in the three youngest somatic cells (arrows), whereas apical PAR-3 is present in several older somatic cells (arrowheads in H).

unlikely that lateral adhesion was disrupted by transgene overexpression of the PAR proteins because the same transgenes did not disrupt adhesion when crossed into otherwise wild-type embryos (Table 1).

Cell-adhesion defects in *par(ZF1)* embryos could result from the mislocalization of adhesive proteins that normally localize to the basolateral surfaces where cells contact other cells. HMR-1, the sole *C. elegans* homolog of E-cadherin, is found in wild-type early embryos exclusively at basolateral surfaces, where it colocalizes with HMP-1/α-catenin and HMP-2/β-catenin (Costa et al., 1998). However both HMR-1 and HMP-1 were localized normally to the basolateral surfaces of all *par-3(ZF1)* embryos examined (Fig. 3E and data not shown). LAD-1, the *C. elegans* homolog of L1CAM, is believed to have a role in cell adhesion and has been reported to localize to the basolateral surfaces of some embryonic cells (Chen et al., 2001). However, LAD-1 was not restricted to the basolateral surfaces of early embryonic cells in wild-type embryos, and this distribution did not change in *par-3(ZF1)* embryos (data not shown).

The first cells to ingress during gastrulation are the two endodermal precursors. The endodermal precursors move from the ventral surface into the interior, beginning ~90 minutes after the first cleavage of the embryo (Sulston et al., 1983). During ingression, neighboring cells spread across the apical surfaces of the endodermal precursors (Lee and Goldstein, 2003; Nance and Priess, 2002). We found that the ingression of the endodermal precursors in *par(ZF1)* embryos was markedly slower than wild-type endodermal precursors. For example, at a time when wild-type endodermal precursors had moved 2±1.2 μm (n=5) away from the ventral surface, the endodermal precursors in *par-3(ZF1)* embryos had either not moved or moved only 0.4±0.5 μm (n=6, P<0.05). The endodermal precursors in wild-type embryos completed ingression in 23 minutes, which corresponds to a single cell cycle (Table 1, Fig. 6Aa-c, Movie 1A at http://dev.biologists.org/supplemental/). By contrast, the endodermal precursors in *par-3(ZF1)* and *par-6(ZF1)* strains required 51 and 43 minutes to complete ingression, respectively, and invariably divided before ingression was complete (Table 1, Fig. 6Ad-f, Movie 1B at http://dev.biologists.org/supplemental/). Expression of PAR-3$^{ZF1\text{-}GFP}$ or PAR-6$^{ZF1\text{-}GFP}$ in otherwise wild-type embryos did not slow ingression, indicating that the ingression defect was not caused by overexpression of the PAR proteins from the transgenes (Table 1).

Because NMY-2/nonmuscle myosin has been implicated in ingression (see Introduction), we used an *nmy-2::gfp* transgene to examine cells in living embryos. In both wild-type and *par-3(ZF1)* embryos, NMY-2^{GFP} was present at low, uniform levels at the cortices of interphase cells, and concentrated at either the cleavage furrow or midbodies of dividing cells (Fig. 6Bb, arrowhead). In wild-type embryos, the ingressing endodermal precursors showed a progressive enrichment of apical NMY-2^{GFP} as their apical surfaces flattened (Fig. 6Ba-c, Movie 2A at http://dev.biologists.org/supplemental/) (4/4 embryos). By contrast, the endodermal precursors in most *par-3(ZF1)* embryos had no enrichment of apical NMY-2^{GFP} during the period ingression normally occurs and little, if any, flattening of their apical surfaces (Fig. 6Bd-f, Movie 2B at http://dev.biologists.org/supplemental/) (6/7 embryos not enriched, 1/7 enriched slightly). Thus, the slow ingression of the endodermal precursors in *par-3(ZF1)* embryos was associated with a failure to contract their apical surfaces and correlated with reduced levels of apical NMY-2.

Two genes in *C. elegans*, *nmy-2* and *nmy-1*, encode nonmuscle myosin heavy chains. Although *nmy-2* is required for anterior-posterior polarity and cell division, roles for *nmy-1* in the early embryo have not been described (Guo and Kemphues, 1996). Because endodermal cells in *par-3(ZF1)* embryos eventually ingress, we wondered if NMY-1 might compensate for the reduced levels of apical NMY-2. However,

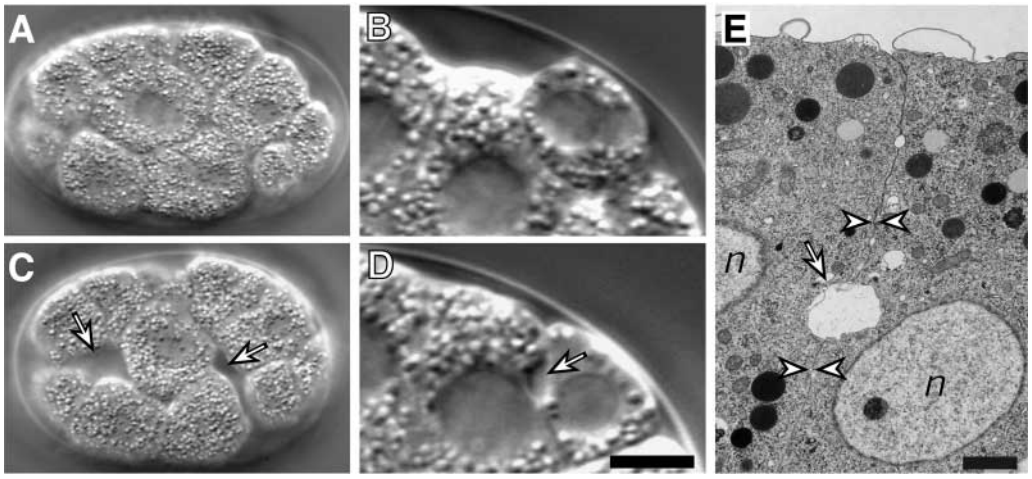

Fig. 5. Lateral cell adhesion. (A,B) Surface (A) and internal (B) images of a wild-type embryo viewed by light microscopy. (C,D) Surface (C) and internal (D) views of a *par-6(ZF1)* embryo. (E) Transmission electron micrograph of a *par-3(ZF1)* embryo. The arrow indicates abnormal intercellular separations. Opposing arrowheads in E indicate contacts between lateral membranes. n, nucleus. Scale bars: 5 μm in D; 1 μm in E.

the pattern of endodermal cell ingression was not altered by depleting NMY-1 by RNA-mediated interference and endodermal cells were internalized at 136±6.7 minutes after the 2-cell stage (*n*=11, compare to *par-3(ZF1)* and wild type in Table 1).

In normal development, ingression of the endodermal precursors is followed by ingression of a group of mesodermal cells that are descendants of an early embryonic cell called MS. Ingression of these MS descendants begins ~1 hour after the E daughters begin their ingression (Nance and Priess, 2002; Sulston et al., 1983). We compared the ingression of a pair of MS descendants (MSaaaa and MSaaap) in wild-type embryos and *par-3(ZF1)* embryos. In wild-type embryos, both cells ingressed ~11 minutes after their birth (11±2 minutes, *n*=5). In each of six *par-3(ZF1)* embryos examined, the same cells had variable defects in ingression. In one embryo, neither cell ingressed during an observation period of two cell cycles. In embryos where the cells eventually ingressed, the first ingression movements were evident 7 minutes later than in wild-type embryos (18±3 minutes after their birth, *n*=5, $P<0.05$). Thus ingressions in both endodermal and mesodermal lineages occur more slowly in *par-3(ZF1)* embryos than in wild-type embryos.

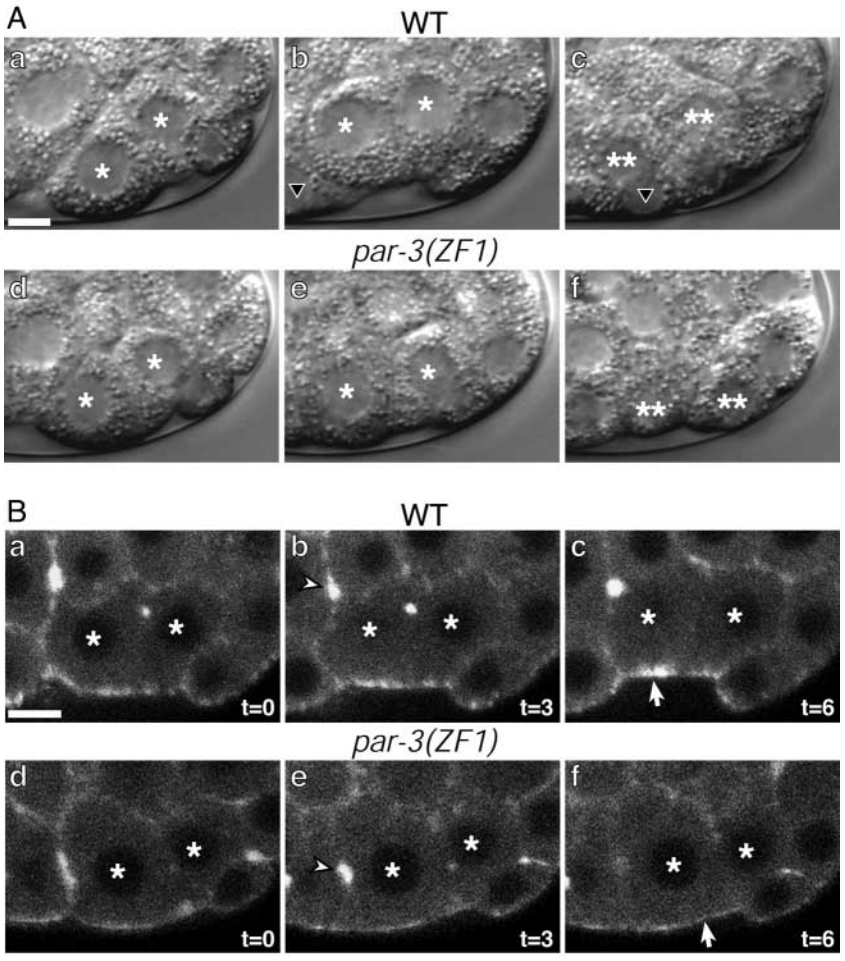

Fig. 6. Ingression of the endodermal precursors. (A) Images from video recordings of the ingression of the E daughters, the endodermal precursors. The focal plane is through the center of the embryo. (a) 24-cell stage. The E daughters (nuclei indicated by single asterisks) are present on the surface of the embryo. (b) 28-cell stage. The E daughters have moved toward the interior of the embryo (top). (c) 46-cell stage. The E daughters have entered the body cavity and divided into the E granddaughters (double asterisks indicate the two visible granddaughters). Neighboring cells (triangle) cover the site of ingression. (d-f) Comparable stages of *par-3(ZF1)* embryos, labeled as above. Note that the E granddaughters remain on the surface of the embryo in f. (B) Confocal images of NMY-2^{GFP} in living embryos during the early stages of ingression, labels as above. The arrowheads in b,e indicate levels of NMY-2^{GFP} in the midbodies of dividing cells; arrows in c and f show the apical surfaces of the E daughters. Time points in minutes are indicated in the lower right-hand corner of each panel; *t*=0 was the 26-cell stage just after the MS(2) to MS(4) division. Scale bars: 5 μm.

Discussion

ZF1-mediated removal of maternal PAR proteins

In *C. elegans*, many maternally expressed gene products perdure over several cell cycles and some can persist throughout embryogenesis into larval stages (Swanson and Riddle, 1981). Delineating when such products function often requires the availability of temperature-sensitive mutant alleles of the protein. We have taken an alternative approach to selectively removing PAR proteins by exploiting a protein degradation system that normally removes the PIE-1 protein from somatic cells. We have shown that fusing the ZF1 domain of PIE-1 to the PAR proteins does not impair PAR functions at the 1-cell stage of embryogenesis when they play a crucial role in establishing anterior-posterior asymmetry. However, the PAR^{ZF1} proteins disappear in the somatic precursor cells after the 4-cell stage and remain absent until late development when the *par* genes are transcribed by the embryo. This technique should prove useful for examining additional maternal proteins that are implicated in early asymmetry, and for analyzing somatic functions of proteins that are expressed in both somatic and germline precursors.

De novo establishment of apicobasal asymmetry within early embryonic cells

During the 4-cell stage of embryogenesis, the PAR proteins undergo a dramatic redistribution along the apicobasal axis. Our results indicate that recruitment of PAR-3 to the apical cortex is a key step in this redistribution, analogous to previous observations on the role of PAR-3 at the 1-cell stage (Watts et al., 1996; Tabuse et al., 1998). We showed that PAR-3 localization to the apical cortex occurs independently of PAR-6 (this study) and PAR-2 (Nance and Priess, 2002). Moreover, PAR-3 localization is crucial for recruiting PAR-6 and PKC-3 to the apical cortex, and restricting PAR-2 to basolateral surfaces. Localization of PAR-3 to the apical cortex is not sufficient for the colocalization of PAR-6 and PKC-3: PAR-6 does not colocalize with apical PAR-3 in *pkc-3(RNAi)* embryos (J.N., E.M.M. and J.R.P., unpublished), and PKC-3 does not colocalize with apical PAR-3 in *par-6(ZF1)* embryos. Thus both PAR-6 and PKC-3 must be present for either protein to associate with apical PAR-3. Biochemical studies of PAR-3, PAR-6 and PKC-3 homologs in mammalian cells have shown that these proteins can bind to one another directly (Joberty et al., 2000; Lin et al., 2000), indicating that interactions between all three proteins might be necessary to stabilize a complex with apical PAR-3.

How is PAR-3 recruited to the apical cortex? Our previous experiments with recombined embryonic cells demonstrated that PAR-3 is excluded from surfaces that are in contact with neighboring cells (Nance and Priess, 2002). Thus, in a normal embryo PAR-3 would be restricted to the contact-free, apical surface. We have shown here that the exclusion of PAR-3 from contact surfaces is not dependent on the presence of PAR-3 in the neighboring cells. First, *par-3(ZF1)* embryos can contain young somatic cells with apically restricted $PAR\text{-}3^{ZF1\text{-}GFP}$ that are adjacent to older somatic cells that lack $PAR\text{-}3^{ZF1\text{-}GFP}$. Second, wild-type cells that are recombined with *par-3* mutant cells correctly localize PAR-3 to their contact-free surfaces. In normal development, PAR-3 must distinguish the apical surface from contact surfaces at each cell cycle because PAR-3 dissociates from and reassociates with the apical cortex before and after each cell division, respectively. In principle, non-PAR proteins could define a location on the apical surface that is maintained during cell division. However, because there is natural variability in cell contacts during cell division, and because our cell recombination experiments show that the apicobasal axis is not fixed (Nance and Priess, 2002), we favor the hypothesis that the apical surface is redefined after each of the early cell divisions.

PAR proteins and cell adhesion

The observation that PAR-3 is excluded from contact surfaces indicates that proteins that are involved in cell adhesion either directly or indirectly influence PAR-3 localization. In a reciprocal manner, the apical PAR-3 complex appears to either directly or indirectly modulate cell adhesion. We have shown that *par(ZF1)* embryos can develop prominent gaps between the lateral surfaces of cells, whereas these surfaces are tightly adherent in normal embryos. Similarly, embryo culture experiments have shown that apical surfaces have the potential to adhere on contact with other cells (Nance and Priess, 2002). Thus, the apical PAR-3 complex might concentrate or modify adhesive factors at the apical and adjacent lateral surfaces. Alternatively, the apical PAR complex might direct the vectorial transport to the basal surface of proteins that inhibit cell adhesion; such proteins would mislocalize to lateral surfaces in *par(ZF1)* embryos. By analogy, an apical PAR complex in *Drosophila* neuroblasts directs the localization of the Miranda protein to the opposite end of the cell (reviewed by Doe and Bowerman, 2001).

Because cell separations occur between many different types of cells in *par(ZF1)* embryos, they appear to be caused by a general defect in cell-cell adhesion. This defect is unlikely to result from a failure to transcribe the genes required for cell adhesion because similar separations are not observed when transcription is inhibited during the early cleavage stages (Nance and Priess, 2002). Thus, we favor the hypothesis that PAR proteins regulate either the localization or activity of maternally provided proteins that have roles in cell adhesion. Maternally expressed HMR-1/E-cadherin associates with HMP-1/α-catenin and HMP-2/β-catenin at the basolateral surfaces of embryonic cells (Costa et al., 1998). However, we observed that both HMR-1 and HMP-1 localize properly in *par-3(ZF1)* embryos. Depletion of HMR-1 or HMP-1 does not lead to noticeable defects in the adhesiveness of the early embryonic cells (Costa et al., 1998), indicating that additional adhesive proteins remain to be identified.

Role of the PAR proteins in gastrulation

Defects in cell adhesion could contribute to the abnormally slow cell ingressions observed in *par(ZF1)* embryos. When an ingressing cell separates from its neighbors at the surface of a normal embryo, a transient gap is created that is closed by the rapid spreading of neighboring cells. This spreading presumably is mediated by lateral adhesion between the newly exposed surfaces of the neighboring cells. Thus, adhesion between the neighboring cells might exert a squeezing force on the ingressing cell that contributes to the normal speed of ingression.

Defects in apical contraction are a second likely cause of the slowed cell ingressions of *par(ZF1)* embryos. In normal

embryos, NMY-2/nonmuscle myosin concentrates at the apical cortex of ingressing cells, reaching a level comparable to that found in the cleavage furrows of dividing cells (Nance and Priess, 2002 and this study). The apical contraction of an ingressing cell could concentrate a fixed, but initially dispersed, population of cortical NMY-2, and lead to an apparent increase in the level of NMY-2. However, membrane-associated proteins such as LAD-1 do not show a similar behavior during cell ingression, raising the possibility that additional NMY-2 is recruited to the apical surfaces of ingressing cells (Chen et al., 2001) (J.N., E.M.M. and J.R.P., unpublished). Irrespective of the mechanism by which NMY-2 is concentrated in normal ingression, this concentration is either markedly reduced or does not occur in *par(ZF1)* embryos. Because myosin activity is essential for apical contraction and ingression (Lee and Goldstein, 2003), failure to either concentrate or activate NMY-2 is likely to lead to defects in ingression.

Why doesn't cell ingression fail completely in the *par(ZF1)* embryos? It is possible that a small but significant amount of $PAR^{ZF1\text{-}GFP}$ persists in ingressing cells. Although we cannot eliminate this possibility, the residual level would have to be below the level of detection of immunocytochemistry using antibodies against either GFP or the various PAR proteins. Moreover, all of the lines of transgenic animals we generated had identical defects in ingression despite considerable variation in their initial level of $PAR^{ZF1\text{-}GFP}$ at the 1-cell stage. A second possibility is that the low level of NMY-2 remaining at the apical surface is sufficient for a weak contraction and slow ingression. It is unlikely that NMY-1 functions redundantly with NMY-2 in this process because depleting NMY-1 in *par-3(ZF1)* embryos does not further impair endodermal cell ingression. Last, it is possible that the PAR-dependent concentration of NMY-2 at the apical surface functions primarily to increase the efficiency of an otherwise PAR-independent pathway for ingression. Cells that lack $PAR^{ZF1\text{-}GFP}$ proteins retain at least one apicobasal asymmetry, the basolateral localization of HMR-1/E-cadherin, and basal localization of structures such as lamellipodia or filopodia could contribute to ingression. Studies in other systems have shown that the ARP2/3 complex of proteins functions in the nucleation and branching of microfilaments and that it localizes to the leading edges of crawling cells (reviewed by Higgs and Pollard, 2001). Interestingly, depletion of the *C. elegans* ARP2/3 complex prevents ingression of the endodermal precursors (Severson et al., 2002). Large filopodial-like projections are apparent on the *C. elegans* endodermal precursors after ingression (J.N., E.M.M. and J.R.P., unpublished), however it is not known whether smaller filopodia and lamellipodia are present during ingression. The possibility that multiple mechanisms contribute to cell ingression in *C. elegans* is reminiscent of studies on invagination in *Drosophila*. During *Drosophila* gastrulation, invaginating sheets of cells flatten and contract their apical surfaces, and apical contraction is associated with an apical accumulation of nonmuscle myosin (reviewed by Leptin, 1999). These shape changes are regulated in part by the Folded gastrulation (Fog) signaling pathway. However, mutations that disrupt the Fog pathway slow, but do not prevent, invagination (Costa et al., 1994; Parks and Wieschaus, 1991).

The fact that cell ingressions can be slowed in *par(ZF1)* embryos in *C. elegans* without causing embryonic lethality is surprising given the essentially invariant positions of embryonic cells during normal tissue morphogenesis (Sulston et al., 1983). However, examples of natural variability in cell positions have been documented in wild-type embryos, where the mispositioned cells can migrate to their normal location (Schnabel et al., 1997). In addition, mutations that block cell death result in embryos with mispositioned cells. These embryos develop into viable animals that appear superficially normal, although they have numerous defects in cellular anatomy (White et al., 1991). We do not yet know whether the mispositioned cells in *par(ZF1)* embryos undergo compensatory migrations or whether the resulting animals have anatomical defects that are not apparent by light microscopy.

Cues and roles for PAR asymmetry

C. elegans embryos have at least three distinct periods in which the PAR-3 complex must distinguish different cell surfaces. At the 1-cell stage PAR-3 associates with the anterior surface, and at the 4-cell stage PAR-3 associates with the apical surface. In late embryogenesis PAR-3 is localized asymmetrically in epithelial cells, and the apicobasal axis of the internal epithelia is inverted with respect to that of earlier embryonic cells (Leung et al., 1999; McMahon et al., 2001) (J.N., E.M.M. and J.R.P., unpublished). These localization patterns appear to be specified de novo during each period. Disruption of PAR asymmetry at the 1-cell stage by mutations in *par-2* does not prevent apical localization of PAR-3 after the 4-cell stage (Nance and Priess, 2002). Similarly, we showed that the absence of the PAR-3 complex between the 4-400-cell stages in *par-3(ZF1)* embryos does not prevent the subsequent apical localization of PAR-3 during organogenesis.

The molecular cues used to localize the PAR-3 complex remain to be identified and, at some level, these are likely to vary. For example, sperm position and cell contacts specify polarity at the 1- and 4-cell stages, respectively. Although the mechanism of PAR localization has not been studied extensively in the epithelial cells of *C. elegans*, genetic studies in *Drosophila* have identified homologs of proteins in the *C. elegans* PAR-3 complex that regulate apicobasal polarity in epithelial cells. E-cadherin-mediated cell adhesion is required for apical PAR-3 complex localization in *Drosophila* epithelial cells (Bilder et al., 2003), whereas HMR-1/E-cadherin is not essential for PAR-3 complex asymmetry at either the 1-cell or 4-cell stage in *C. elegans* (Costa et al., 1997; Nance and Priess, 2002). Apical localization of the PAR-3 complex in *Drosophila* epithelia is antagonized by a basolateral complex of proteins that includes Discs large and Scribble (Bilder et al., 2003; Tanentzapf and Tepass, 2003). The *C. elegans* homologs of the latter proteins, DLG-1/Discs large and LET-413/Scribble, are expressed in epithelial cells, and depletion of these proteins causes epithelial defects (reviewed by Knust and Bossinger, 2003). However, these proteins do not appear to function in apicobasal polarity of early embryonic cells because they are either not expressed in the early embryo (DLG-1) or are not required for apical localization of PAR-3 (*let-413*) (J.N., E.M.M. and J.R.P., unpublished). Thus, identifying the molecular basis of cell-contact-dependent PAR localization remains an important goal for future studies on apicobasal PAR asymmetry.

We thank Lihsia Chen, Andy Fire, Ben Leung and Susan Strome for providing antisera and plasmids, and Ken Kemphues for generously supplying PAR antibodies. We thank Judy Groombridge and Bobbie Schneider for assistance with electron microscopy, Liz Wayner for antibody production, and Rafal Ciosk and Susan Parkhurst for providing helpful comments on the manuscript. Some of the nematode strains used in this study were provided by the *Caenorhabditis* Genetics Center, which is funded by the NIH National Center for Research Resources. J.N. is supported by Postdoctoral Fellowship Grant # PF-02-007-01-DCC from the American Cancer Society, E.M.M. is supported by the NIH (NIGMS 5P50 GM66050-02) and J.R.P. is supported by the Howard Hughes Medical Institute.

References

Bilder, D., Schober, M. and Perrimon, N. (2003). Integrated activity of PDZ protein complexes regulates epithelial polarity. *Nat. Cell Biol.* **5**, 53-58.

Boyd, L., Guo, S., Levitan, D., Stinchcomb, D. T. and Kemphues, K. J. (1996). PAR-2 is asymmetrically distributed and promotes association of P granules and PAR-1 with the cortex in *C. elegans* embryos. *Development* **122**, 3075-3084.

Brenner, S. (1974). The genetics of *Caenorhabditis elegans*. *Genetics* **77**, 71-94.

Cassata, G., Kagoshima, H., Prétôt, R. F., Aspöck, G., Niklaus, G. and Bürglin, T. R. (1998). Rapid expression screening of *Caenorhabditis elegans* homeobox open reading frames using a two-step polymerase chain reaction promoter-*gfp* reporter construction technique. *Gene* **212**, 127-135.

Chen, L., Ong, B. and Bennett, V. (2001). LAD-1, the *Caenorhabditis elegans* L1CAM homologue, participates in embryonic and gonadal morphogenesis and is a substrate for fibroblast growth factor receptor pathway-dependent phosphotyrosine-based signaling. *J. Cell Biol.* **154**, 841-855.

Cheng, N. N., Kirby, C. M. and Kemphues, K. J. (1995). Control of cleavage spindle orientation in *Caenorhabditis elegans*: the role of the genes *par-2* and *par-3*. *Genetics* **139**, 549-559.

Costa, M., Wilson, E. T. and Wieschaus, E. (1994). A putative cell signal encoded by the *folded gastrulation* gene coordinates cell shape changes during *Drosophila* gastrulation. *Cell* **76**, 1075-1089.

Costa, M., Draper, B. W. and Priess, J. R. (1997). The role of actin filaments in patterning the *Caenorhabditis elegans* cuticle. *Dev. Biol.* **184**, 373-384.

Costa, M., Raich, W., Agbunag, C., Leung, B., Hardin, J. and Priess, J. R. (1998). A putative catenin-cadherin system mediates morphogenesis of the *Caenorhabditis elegans* embryo. *J. Cell Biol.* **141**, 297-308.

Doe, C. Q. and Bowerman, B. (2001). Asymmetric cell division: fly neuroblast meets worm zygote. *Curr. Opin. Cell Biol.* **13**, 68-75.

Etemad-Moghadam, B., Guo, S. and Kemphues, K. J. (1995). Asymmetrically distributed PAR-3 protein contributes to cell polarity and spindle alignment in early *C. elegans* embryos. *Cell* **83**, 743-752.

Guo, S. and Kemphues, K. J. (1995). *par-1*, a gene required for establishing polarity in *C. elegans* embryos, encodes a putative Ser/Thr kinase that is asymmetrically distributed. *Cell* **81**, 611-620.

Guo, S. and Kemphues, K. J. (1996). A non-muscle myosin required for embryonic polarity in *Caenorhabditis elegans*. *Nature* **382**, 455-458.

Higgs, H. N. and Pollard, T. D. (2001). Regulation of actin filament network formation through ARP2/3 complex: activation by a diverse array of proteins. *Annu. Rev. Biochem.* **70**, 649-676.

Hodgkin, J. (1997). Genetics. In *C. elegans II* (ed. D. L. Riddle, T. Blumenthal, B. J. Meyer and J. R. Priess), pp. 881-1048. Plainview, NY: Cold Spring Harbor Laboratory Press.

Hodgkin, J., Horvitz, H. R. and Brenner, S. (1979). Nondisjunction mutants of the nematode *C. elegans*. *Genetics* **91**, 67-94.

Hung, T. J. and Kemphues, K. J. (1999). PAR-6 is a conserved PDZ domain-containing protein that colocalizes with PAR-3 in *Caenorhabditis elegans* embryos. *Development* **126**, 127-135.

Joberty, G., Petersen, C., Gao, L. and Macara, I. G. (2000). The cell-polarity protein Par6 links Par3 and atypical protein kinase C to Cdc42. *Nat. Cell Biol.* **2**, 531-539.

Kawasaki, I., Shim, Y. H., Kirchner, J., Kaminker, J., Wood, W. B. and Strome, S. (1998). PGL-1, a predicted RNA-binding component of germ granules, is essential for fertility in *C. elegans*. *Cell* **94**, 635-645.

Kemphues, K. J., Priess, J. R., Morton, D. G. and Cheng, N. (1988). Identification of genes required for cytoplasmic localization in early *C. elegans* embryos. *Cell* **52**, 311-320.

Kemphues, K. J. and Strome, S. (1997). Fertilization and establishment of polarity in the embryo. In *C. elegans II* (ed. D. L. Riddle, T. Blumenthal, B. J. Meyer and J. R. Priess), pp. 335-359. Plainview, NY: Cold Spring Harbor Laboratory Press.

Knust, E. and Bossinger, O. (2003). Composition and formation of intercellular junctions in epithelial cells. *Science* **298**, 1955-1959.

Lee, J.-Y. and Goldstein, B. (2003). Mechanisms of cell positioning during *C. elegans* gastrulation. *Development* **130**, 307-320.

Leptin, M. (1999). Gastrulation in *Drosophila*: the logic and the cellular mechanisms. *EMBO J.* **18**, 3187-3192.

Leung, B., Hermann, G. J. and Priess, J. R. (1999). Organogenesis of the *Caenorhabditis elegans* intestine. *Dev. Biol.* **216**, 114-134.

Lin, D., Edwards, A. S., Fawcett, J. P., Mbamalu, G., Scott, J. D. and Pawson, T. (2000). A mammalian PAR-3-PAR-6 complex implicated in Cdc42/Rac1 and aPKC signalling and cell polarity. *Nat. Cell Biol.* **2**, 540-547.

Maduro, M. and Pilgrim, D. (1995). Identification and cloning of *unc-119*, a gene expressed in the *Caenorhabditis elegans* nervous system. *Genetics* **141**, 977-988.

Maduro, M. F. and Rothman, J. H. (2002). Making worm guts: the gene regulatory network of the *Caenorhabditis elegans* endoderm. *Dev. Biol.* **246**, 68-85.

McMahon, L., Legouis, R., Vonesch, J. L. and Labouesse, M. (2001). Assembly of *C. elegans* apical junctions involves positioning and compaction by LET-413 and protein aggregation by the MAGUK protein DLG-1. *J. Cell Sci.* **114**, 2265-2277.

Mello, C. and Fire, A. (1995). DNA transformation. In *Caenorhabditis elegans: Modern Biological Analysis of an Organism*. Vol. 48 (ed. H. F. Epstein and D. C. Shakes), pp. 451-482. San Diego: Academic Press.

Mello, C. C., Schubert, C., Draper, B., Zhang, W., Lobel, R. and Priess, J. R. (1996). The PIE-1 protein and germline specification in *C. elegans* embryos. *Nature* **382**, 710-712.

Müller, H.-A. J. and Wieschaus, E. (1996). *armadillo*, *bazooka*, and *stardust* are critical for early stages in formation of the zonula adherens and maintenance of polarized blastoderm epithelium in *Drosophila*. *J. Cell Biol.* **134**, 149-163.

Nance, J. and Priess, J. R. (2002). Cell polarity and gastrulation in *C. elegans*. *Development* **129**, 387-397.

Parks, S. and Wieschaus, E. (1991). The *Drosophila* gastrulation gene *concertina* encodes a Gα-like protein. *Cell* **64**, 447-458.

Pellettieri, J. and Seydoux, G. (2002). Anterior-posterior polarity in *C. elegans* and *Drosophila*–PARallels and differences. *Science* **298**, 1946-1950.

Petronczki, M. and Knoblich, J. A. (2001). DmPAR-6 directs epithelial polarity and asymmetric cell division of neuroblasts in *Drosophila*. *Nat. Cell Biol.* **3**, 43-49.

Praitis, V., Casey, E., Collar, D. and Austin, J. (2001). Creation of low-copy integrated transgenic lines in *Caenorhabditis elegans*. *Genetics* **157**, 1217-1226.

Priess, J. R. and Hirsh, D. I. (1986). *Caenorhabditis elegans* morphogenesis: The role of the cytoskeleton in elongation of the embryo. *Dev. Biol.* **117**, 156-173.

Reese, K. J., Dunn, M. A., Waddle, J. A. and Seydoux, G. (2000). Asymmetric segregation of PIE-1 in *C. elegans* is mediated by two complementary mechanisms that act through separate PIE-1 protein domains. *Mol. Cell* **6**, 445-455.

Schnabel, R., Hutter, H., Moerman, D. and Schnabel, H. (1997). Assessing normal embryogenesis in *Caenorhabditis elegans* using a 4D microscope: variability of development and regional specification. *Dev. Biol.* **184**, 234-265.

Severson, A. F., Baillie, D. L. and Bowerman, B. (2002). A formin homology protein and a profilin are required for cytokinesis and Arp2/3-independent assembly of cortical microfilaments in the early *Caenorhabditis elegans* embryo. *Curr. Biol.* **12**, 2066-2075.

Sulston, J. E., Schierenberg, E., White, J. G. and Thomson, J. N. (1983). The embryonic cell lineage of the nematode *Caenorhabditis elegans*. *Dev. Biol.* **100**, 64-119.

Swanson, M. M. and Riddle, D. L. (1981). Critical periods in the development of the *Caenorhabditis elegans* dauer larva. *Dev. Biol.* **84**, 27-40.

Tabuse, Y., Izumi, Y., Piano, F., Kemphues, K. J., Miwa, J. and Ohno, S. (1998). Atypical protein kinase C cooperates with PAR-3 to establish embryonic polarity in *Caenorhabditis elegans*. *Development* **125**, 3607-3614.

Tanentzapf, G. and Tepass, U. (2003). Interactions between the *crumbs*,

lethal giant larvae and *bazooka* pathways in epithelial polarization. *Nat. Cell Biol.* **5**, 46-52.

Tenenhaus, C., Schubert, C. and Seydoux, G. (1998). Genetic requirements for PIE-1 localization and inhibition of gene expression in the embryonic germ lineage of *Caenorhabditis elegans*. *Dev. Biol.* **200**, 212-224.

Watts, J. L., Etemad-Moghadam, B., Guo, S., Boyd, L., Draper, B. W., Mello, C. C., Priess, J. R. and Kemphues, K. J. (1996). *par-6*, a gene involved in the establishment of asymmetry in early *C. elegans* embryos, mediates the asymmetric localization of PAR-3. *Development* **122**, 3133-3140.

Wayner, E. A. and Carter, W. G. (1987). Identification of multiple cell adhesion receptors for collagen and fibronectin in human fibrosarcoma cells possessing unique alpha and common beta subunits. *J. Cell Biol.* **105**, 1873-1884.

White, J. G., Southgate, E. and Thomson, J. N. (1991). On the nature of undead cells in the nematode *Caenorhabditis elegans*. *Philos. Trans. R. Soc. Lond.* **331**, 263-271.

Wodarz, A., Ramrath, A., Grimm, A. and Knust, E. (2000). *Drosophila* atypical protein kinase C associates with Bazooka and controls polarity of epithelia and neuroblasts. *J. Cell Biol.* **150**, 1361-1374.